Published in final edited form as:
Biochim Biophys Acta. 2007 January ; 1769(1): 61–75.

Isolation, Sequencing, and Functional Analysis of the TATA-less Murine *ATPase II* Promoter and Structural Analysis of the *ATPase II* Gene*

Tomasz Sobocki[§], **Farah Jayman**[§,¥], **Malgorzata B. Sobocka**[¶], **Jonathan D. Marmur**[¶], and **Probal Banerjee**

Department of Chemistry and the CSI/IBR Center for Developmental Neuroscience, City University of New York at the College of Staten Island, Staten Island, NY, 10314

¶*Department of Medicine, SUNY Downstate Medical Center, Brooklyn, NY,10203.*

Abstract

The P-type Mg^{2+}-ATPase, termed ATPase II (Atp8a1), is a putative aminophospholipid transporting enzyme, which helps to maintain phospholipid asymmetry in cell membranes. In this project we have elucidated the organization of the mouse *ATPase II* gene and identified its promoter. Located within chromosome 5, this *gene* spans about 224 kb and consists of 38 exons, three of which are alternatively spliced (exons 7, 8 and 16), giving rise to two transcript variants. Translation of these transcripts results in two ATPase II isoforms (1 and 2) composed of 1164 and 1149 amino acids, respectively. Using RNA ligase-mediated rapid amplification of cDNA ends (RLM-RACE) we identified multiple transcription start sites (TSS) in messages obtained from heart, lung, liver, and spleen. The mouse *ATPase II* promoter is TATA-less and lacks a consensus initiator sequence. Luciferase reporter analysis of full and core promoters revealed strong activity and little cell type specificity, possibly because more flanking, regulatory sequences are required to cause such tissue specificity. In the neuronal HN2, N18, SN48 cells and the NIH3T3 fibroblast cells, but not in the B16F10 melanoma cells, the core promoter (-318/+193 with respect to the most common TSS) displayed significantly higher activity than the full promoter (-1026/+193). Serial 5′ deletion of the core promoter revealed significant cell type-specific activity of the fragments, suggesting differential expression and use of transcription factors in the five cell lines tested. Additionally distribution of the TSS was organ specific. Such observations suggest tissue-specific differences in transcription initiation complex assembly and regulation of *ATPase II* gene expression. Information presented here form the groundwork for further studies on the expression of this gene in apoptotic cells.

Keywords

P-type ATPase; promoter; mouse ATPase II; apoptosis; aminophospholipid translocase

*The sequence data presented in this article have been entered into the EMBL/GenBank database under accession numbers DQ503476-DQ503480.

Correspondences should be addressed to: Probal Banerjee, Ph.D., Professor, Department of Chemistry and the CSI/IBR Center for Developmental Neuroscience, The City University of New York at The College of Staten Island, Staten Island, NY, 10314. Phone: (718) 982-3938. FAX (718) 982-3944. Email address: banerjee@mail.csi.cuny.edu

§These two authors contributed equally.

¥Presently, Dr. Farah Jayman, National Institute on Aging, Gerontology Research Center, Laboratory of Cellular and Molecular Biology, Room 1C14 / Box 12; 5600 Nathan Shock Drive, Baltimore, MD 21224, USA.

1. Introduction

The distribution of phospholipids in the animal cell plasma membrane is not random. Instead, the aminophospholipids, phosphatidylserine (PS) and phosphatidylethanolamine (PE) are commonly present in the inner leaflet of the phospholipid bilayer whereas zwitterionic phospholipids, phosphatidylcholine (PC) and sphingomyelin are present in the outer leaflet [1-3]. Polar head groups present in plasma membrane lipids cannot cross a hydrophobic membrane interior freely and for this reason a system of sophisticated proteins evolved in eukaryotic cells to facilitate such transbilayer movements of phospholipids (reviewed in [4]).

At least three distinct protein-based activities are involved in the regulation of membrane lipid asymmetry and in generation and maintenance of the aminophospholipid gradient. These are energy dependent inwardly directed (‘flippases’) and outwardly directed transporters (‘floppases’) as well as energy independent bi-directional transporters (‘scramblases’) [reviewed in [3]]. Flippases are highly specific for PS and are responsible for sequestering it from the cell surface. Floppases are, with a few exceptions, nonspecific toward phospholipids head groups and have been associated with the ABC (ATP binding cassette) class of membrane transporters. Scramblases are also nonselective toward head groups and play a major role in randomizing the distribution of the newly synthesized phospholipids [2,5,6]. The interplay between these specific and nonspecific transporters result in generation and maintenance of asymmetry and gradient phospholipids distribution, which is responsible for multiple morphological and functional characteristics of living cells as well as homeostasis that is essential for their survival [reviewed in [1]].

As mentioned earlier, phosphatidylserine (PS) is normally sequestered to the inner leaflet of the plasma membrane due to the action of a flippase [1,7-9], which is chemically named as aminophospholipid translocase (APTL) or aminophospholipid flippase [1-3]. During programmed cell death, the loss of the aminophospholipid asymmetry, which is typical for healthy cells, leads to the appearance of PS on the cell surface. This externalization of PS serves as a signal for phagocytosis of apoptotic lymphocytes, neutrophils, and neuronal cells by macrophages and microglia [6-8,10]. Our earlier studies to analyze the mechanism of this PS externalization established that the enzymatic activity of APTL is inhibited during apoptosis, which could be the prime reason for the observed PS externalization [10].

Several lines of experimental evidence have been provided linking the PS-translocating enzymatic activity of APTL to the ATPase activity of the mammalian enzyme ATPase II [aminophospholipid transporter, class I, type 8A, member 1 (Atp8a1)], first cloned from bovine chromaffin granules [11]. Both APTL activity and the ATPase II molecule require PS and Mg^{++} to carry out ATP hydrolysis. Furthermore, both the activities are inhibited by vanadate (VO^{2-}_4) and N-ethylmaleimide. Both activities are also inhibited in the presence of increased intracellular Ca^{2+} concentration (>0.2 μM) and selective depletion of intracellular Ca^{2+}, which causes an inhibition of the Ca^{2+}-ATPase, leaves APTL and ATPase II completely active [3, 12]. Of mammalian ATPase II cDNAs, in addition to the bovine ATPase II cDNA, its murine and human homologs have been cloned [13,14]. A yeast strain with a mutant gene (Drs2), which is homologous to the mammalian *ATPase II* gene, showed inhibited translocation of PS across the plasma membrane [15]. Drs2 is one of sixteen yeast genes arranged in five classes and bearing characteristics of P-type ATPases. The bovine and murine ATPase II proteins are most homologous to the yeast gene product Drs2 [16].

Our earlier studies demonstrated that overexpression of mouse ATPase II cDNA [14] in the mouse hippocampus-derived hybrid neuroblastoma (HN2) causes an increase in APTL activity measured by PS translocation [17,18]. In the same cell line, overexpression of ATPase II rendered cells insensitive to stress-induced inhibition of APTL activity, which is otherwise

inhibited in the cells expressing only endogenous ATPase II. ATPase II is a member of a type-4 subfamily of the P-type ATPases. This evolutionarily conserved superfamily of P-type of ATPase is widely expressed in eukaryotes and prokaryotes and consists of 5 subfamilies. The type-4 subfamily is expressed only in the higher eukaryotes while the members of the type-3 subfamily are almost exclusively found in plants and fungi. The core of a typical P-type ATPase contains a P-type signature sequence DKTGT[L,I,V,M][T,I,S] and also harbors 10 putative transmembrane domains. Its molecular weight ranges from 70-150 kDa. With an exception of the type-4 subfamily, which includes proteins believed to translocate phospholipids, members of four other subfamilies are involved in translocating cations across the plasma membrane. The aspartic acid residue (D) in the P-type signature sequence accepts γ-phosphate from ATP during a phosphorylation cycle and this phosphotransfer is an essential driving force behind all P-type ATPases mediated transport [19,20].

Tissue specific expression of ATPases have been well characterized [14,21]. Surprisingly, among the multiple members of P-type ATPases known so far [11,16,19,21], the promoters for only a few P-type ATPase genes has been identified. Among others, these genes are, respectively, human *ATPase II* and *ATPase7B* [22,23]. *ATPase7B* and the closely related homolog *ATPase7A* yield homologous, copper transporting, P-type ATPases. A defect in *ATPase7A* results in Menke's disease and malfunction of the *ATPase7B* gene product leads to Wilson disease [23-27]. Menkes disease is associated with overall copper deficiency due to impaired export of copper from intestinal cells. Wilson's disease, in contrast, is caused by copper accumulation predominantly in the liver, brain, and kidneys. Previous studies by our research group characterized the promoter and the 5′UTR in human P-type aminophospholipid transporting *ATPase II* [22]. In the present study we report isolation and characterization of mouse *ATPase II* promoter as well as its 5′UTRs from various organs and compare and contrast its function with those of the human homolog. Intriguingly, notwithstanding significant homology between them, some prominent differences exist in the organization of mouse and human genes and their promoter elements, which underscore the importance of the current study.

2. Materials and Methods

2.1. Reagents

The GeneRacer™ Kit for full-length, RNA ligase-mediated rapid amplification of 5′ ends (RLM-RACE), the TOPO-TA™ Cloning Kit and Thermozyme™ thermostable DNA polymerase, the THERMOSCRIPT™ RT-System, the Platinum® Taq High Fidelity thermostable DNA polymerase, agarose and a dNTPs mixture were purchased from Invitrogen Corporation (Carlsbad, CA). Proteinase K (fungal) was purchased from Invitrogen. Prior to use, proteinase K was dissolved in 10 mM Tris-Cl (pH 7.5)-20 mM $CaCl_2$-50% glycerol and stored in single use aliquots at -20 °C. The QIAprep Miniprep plasmid DNA isolation kit, QIAquick PCR purification kit, QIAquick gel extraction kit, the Effectene™ Transfection Reagent, RNeasy Mini kit including QIAShredder™ columns and on-column DNase digestion kit were purchased from QIAGEN (Valencia, CA). The pGL3-Basic (no promoter) and pGL3-Promoter (SV40 promoter) firefly luciferase reporter plasmids, pRL-TK vector and the Dual Luciferase Reporter (DLR) assay kit were purchased from Promega (Madison, WI).

2.2. Cell Lines

B16F10 mouse melanoma cells were obtained from Dr. Susan Rotenberg (Queens College, Flushing, NY). The mouse hippocampal neuron-derived hybrid neuroblastoma cell line HN2 cells were obtained from the CSI cell depository. N18 (Mouse neuroblastoma cells) were obtained from Dr. Efrain Azmitia, New York University (NY, NY). The SN48.1p cell line was a generous gift from Dr. Paul Albert (University of Ottawa, Ottawa, Canada). All these cells

were cultured in DMEM (Dulbecco's Modified Eagles Medium) containing 10% FBS (Fetal Bovine Serum) and 1% PS (Penicillin-Streptomycin). NIH3T3 cells (generous gift from Dr. Yu-Wen Hwang's lab at the NY State Institute For Basic Research, Staten Island, NY) were cultured with DMEM media containing 10% Calf Serum and 1% PS.

2.3. Organization of the *ATPase II* gene and analysis of the ATPase II isoforms produced as a result of alternative splicing

In order to elucidate the chromosomal organization of the *ATPase II* gene, we compared the sequences of mouse ATPase II cDNAs NM_009727, NM_001038999, U75321, AK220560, AK045367 and AK076388 to Mouse Genome Sequence using the UCSC Genome Browser (http://genome.ucsc.edu/) [28-30]. Data presented in this paper were obtained using the February 2006 assembly, which is the most recent version. Alignment of genomic and cDNA sequences was carried out using ClustalW ([31]; http://www.ebi.ac.uk/clustalw/) or BCM Search Launcher: Multiple Sequence Alignments software package ([32]; http://searchlauncher.bcm.tmc.edu/multi-align/multi-align.html). Wherever necessary, sequences were aligned manually using standard word processing software and visually inspected. Shaded alignments of multiple sequences were obtained using a 3.21 of BOXSHADE software, written by K. Hofmann and M. Baron and available on the web at: http://www.ch.embnet.org/software/BOX_form.html.

2.4. Primer design

In order to select PCR primer sequences of specific length and temperature of annealing, we used the "RAWPRIMER" program (formerly located at: http://alces.med.umn.edu/rawprimer.html, which is no longer available). Primers were analyzed for the absence of stems or hairpin loops using the "Primerdesign" utility (http://www.cybergene.se/primer.html). The primers used in these studies are listed in Table I. Each primer contained either CGG GGT ACC or CTA GCT AGC (KpnI or NheI sites respectively, underlined plus three protecting bases). These restriction sites enabled us to perform directional cloning of the PCR products into the reporter vector pGL3-Basic resulting in a product being cloned in either sense or antisense orientation. All custom primers used in this project were synthesized by Invitrogen. Primers used for amplification of the 5′ cDNA ends: GeneRacer™ 5′ [forward] Primer (GeneRacer 5′F), GeneRacer™ 5′ Nested [forward] Primer (GeneRacer 5′NF) were included in the GeneRacer™ kit.

2.5. DNA Sequencing

The promoter deletion mutants and the 5′RACE products cloned into their respective vectors were sequenced commercially by ACGT, Inc (Wheeler, IL). Each clone was sequenced on both strands at first using the appropriate universal primers. Whenever necessary, additional sequencing using internal primers was carried out until all discrepancies in sequencing data were resolved.

2.6. Searching for the potential promoter region and transcription factor (TF) binding sites in the *ATPase II* Gene

The search for the potential promoter region in the *ATPase II* gene was performed using the GenomatixSuite collection software (Genomatix Software GmbH, Munich, Germany) available at http://www.genomatix.de. The PromoterInspector [33] mammalian promoter prediction software was used to analyze the 5′ end of the *ATPase II* gene for the presence of the potential promoter and the MatInspector professional 7.4.3 [34] to identify the potential TF binding sites. Searches for the potential transcription factor (TF) binding sites present in both human [22] as well as murine *ATPase II* promoters were carried out using DiAlign professional TF Release 3.1.1 (http://www.genomatix.de/online_help/help_dialign/

dialign_TF.html). This program combines alignment of input sequences using multiple alignment program DiAlign ([35,36]; http://www.genomatix.de/online_help/help_dialign/dialign2_help.html#algorithm) with detection of potential TF binding-site matches by MatInspector. The solution parameters for MatInspector were: core similarity of 0.75 and optimized matrix similarity (program's default settings), search for matches to individual transcription factors using ALL vertebrates.lib. DiAlign TF search was carried out to identify common TF matches located in aligned regions and common to both promoter sequences aligned.

2.7. Isolation and Analysis of Mouse *ATPase II* Promoter

The promoter fragments subsequently tested for transcriptional activity were PCR amplified from 100 ng of genomic DNA per sequence amplified. In brief, a 50 μl PCR reaction contained the following: 1 X HiFi buffer, 2 mM $MgSO_4$, 0.2 mM dNTP mix, 1.5 U of Platinum HiFi Taq polymerase, 2.5 μl PCR_x enhancer as well as 2 μM of each forward ('sns') and reverse ('antsns') primer (see Table I). PCR conditions were 96 °C for 2 minutes, 94 °C for 2 minutes, 5 cycles of 96 °C for 45 seconds, 64 °C for 30 seconds, 68 °C for 1 minute, then 28 cycles of 95 °C for 45 seconds, 61 °C for 30 seconds, 68 °C for 1 minute; finally 72 °C for 10 minutes. The promoter fragments amplified were cloned into pCRII-TOPO TA vector and then re-cloned into pGL3 Basic vector in either a sense or antisense orientation with respect to the luciferase reporter gene.

2.8. Isolation of total RNA from mouse organs

Swiss Webster mice were sacrificed by cervical dislocation and immediately dissected. The organs (heart, liver, lung and spleen) were placed in ice-cold PBS prepared using 0.1% diethylpyrocarbonate (DEPC)-treated water and then rinsed and minced into small pieces while still submerged in the solution. Then, the tissues were snap frozen in liquid nitrogen and powdered using mortar and pestle. The pulverized tissue was immediately dissolved in RLT Lysis buffer (a part of the RNeasy kit) and RNA was isolated using the kit. The RNA obtained was subjected to on-column DNAase digestion for 30 min at 23 °C, as detailed in the manufacturer's protocol and the quality of the isolated RNA was verified by formaldehyde/formamide agarose gel electrophoresis.

2.9. Isolation of genomic DNA from mouse tail

Approximately 0.25 cm of the ends of the tails of C57 mice were removed using clean, isopropanol-sterilized sharp blade. Tails were dissolved by overnight incubation at 55 °C in approximately 720 μl of NTE buffer (50 mM Tris-Cl, pH 8.0, 50 mM EDTA, 100 mM NaCl and 1% SDS) buffer containing 0.6 mg/ml Proteinase K. The incubation was carried out in closed Eppendorf tubes on a rotating platform. The small amounts of debris remaining were separated from the supernatant by centrifugation. Each supernatant was subsequently extracted with phenol and then subjected to RNAseA (70 μg/ml) digestion. This was followed by extraction using phenol-chlorophorm-isoamyl alcohol (25:24:1). The genomic DNA was then precipitated by adding an equal volume of isopropanol. The pellet separated by centrifugation was washed with 80% ethanol, air dried to remove the ethanol, and then rehydrated. The concentration and purity of the nucleic acid was tested by absorbance measurements at 260 and 280 nm. The quality of DNA was further tested by agarose gel electrophoresis.

2.10. Transient transfection studies of the *ATPase II* promoter

Transient transfections with *ATPase II* promoter constructs in pGL3Basic (firefly luciferase) and pRL-TK (Renilla luciferase) into the cells used in theses studies were achieved using the Effectene reagent (Qiagen, Valencia, CA) according to the manufacturer's recommendations. In brief, cells grown to 30% confluence in a 24-well plate were washed with serum-free DMEM

and then treated with the following transfection mixture (using a Qiagen transfection kit): Plasmid DNA (200ng per well containing 197.5 ng of promoter construct pDNA plus 2.5 ng pRL-TK) + EC buffer (60 μl) + Enhancer (1.6 μl) were assembled, vortexed briefly and incubated for 5′ at room temperature. Then Effectene (5 μl) was added to the transfection mixture followed by brief vortexing and incubation at room temperature for 10′. Finally, 350 μl of DMEM (10% FBS, 1% PS) was added and mixed. This reagent mix was then added to one well of cells overlayered with 350 μl of DMEM (10% FBS, 1% PS). After 3 h at 37 °C, the medium was replaced with 1 ml of regular growth medium (DMEM plus 10% FBS, 1% PS) and the cells were allowed to grow for 48 h. Next, cells were washed with PBS and lysed in 200 μl 1x Passive lysis buffer included in the DLR assay kit and 20 μl of each lysate was added to 100 μl of luciferase assay reagent II (LARII). After mixing, initial luminescence was measured within 30 sec using a TD20/20 Luminometer (Turner Design, Sunnyvale, CA). Subsequent to the first reading, the sample tube was removed from the luminometer and 100 μl of 'Stop & Glo' Buffer (included by the kit), was added to the mixture of LAR II and lysate. Luminescence from either firefly or Renilla luciferase was measured using the same luminometer. Results were expressed as a ratio of Firefly to Renilla luminescence. All results were normalized to the activity obtained from the pGL3-Promoter vector (i.e the SV40 promoter containing vector with the luciferase reporter gene). Statistical significance of the differences in transcriptional activities of serial deletions was analyzed using ANOVA with Bonferroni Post Hoc Test and the alpha value of 0.05. While analyzing results obtained from different deletion mutants, data from not more than four mutants were compared using ANOVA at one time. This was done to avoid errors that arise when larger sets are compared at a time [38].

2.11. Determination of the transcription starts sites of *ATPase II*

Total RNA samples (5 μg each) obtained from mouse heart, lung, liver and spleen (SwissWebster Mouse), were processed for RLM-RACE using the GeneRacer™ (Invitrogen, CA) kit as detailed in the manufacturer's protocol. The RNA samples were dephosphorylated in the presence of 10 U of calf intestinal phosphatase (CIP) at 50 °C for 1 hour. Following purification of the RNA by ethanol precipitation, the mRNA cap structure was removed by treating the dephosphorylated RNA with 0.5 U of tobacco acid pyrophosphatase (TAP). The decapped mRNA was purified and then ligated in the presence of T4 ligase (5U) to an adapter RNA oligonucleotide sequence that was specific for both the GeneRacer 5′ Primer and the GeneRacer 5′ Nested primer. An aliquot of the purified ligation product, containing approximately 2 μg of RACE-ready RNA, was reverse transcribed in the presence of an oligo dT primer using 200 U of SuperScript™ III RT (Invitrogen, CA). The product was subsequently treated with 2 U of RNase H at 37 °C for 20 minutes and then the cDNA product was used immediately for PCR amplification. PCR amplification was performed first with the GeneRacer 5′ Primer and *ATPase II*-specific primer NM_009727.exon3 (Table I). PCR conditions were 94 °C/2 minutes followed by 5 cycles of 94 °C/30 seconds, 62 °C/30 seconds, 68 °C/2 minutes, then 5 cycles of 94 °C/30 seconds, 60 °C/30 seconds, 68 °C/2 minutes, and 25 cycles of 94 °C/30 seconds, 58 °C/30 seconds, 68 °C/2 minutes, and then finally an extension at 72 °C for 10 minutes. An aliquot containing 4% of the primary PCR product was then reamplified using the GeneRacer 5′ Nested Primer and a second *ATPase II*-specific primer NM_009727.exon2 (Table I). The conditions for PCR were 94 °C/2 minutes, followed by 25 cycles of 94 °C/30 seconds, 63°C/ 30 seconds, 68 °C/1 minute, and a final extension at 68 °C for 10 minutes. The products obtained were analyzed on agarose gels. The expected size of such products were exactly 30-bp larger due to the presence at the 5′ ends of the products an additional stretch of oligodeoxynucleotide originating from a part of the reverse transcribed GeneRacer RNA oligonucleotide sequence. Gel-purified products were cloned into pCR4-TOPO vector and sequenced. Two independently obtained clones from each tissue were analyzed.

3. Results

3.1. Identification of the putative mouse ATPase II promoter and analysis of the transcriptional activity of three of its segments

We have previously identified and characterized human *ATPase II* promoter [22]. Using information on the human *ATPase II* promoter and collecting details on mouse ATPase II mRNA sequences and expressed sequence tags (ESTs) from public databases we undertook the current project. Our searches using BLAST [39] and BlastZ [40] initially identified fragments of the putative mouse *ATPase II* promoter as part of the Mus musculus WGS supercontig Mm5_WIFeb01_77 (NW_000229) within mouse chromosome 5 (Sobocka, unpublished). In addition, sequences with high GC content, which are often associated with the presence of a promoter [41], were identified in the region immediately upstream of the translation start site. The CpG island in mouse *ATPase II* gene extends between bases 68,126,255 and 68,126,763 on the negative strand of chromosome 5, band 5qC3.1. This corresponds to the 3′ part of the putative *ATPase II* promoter, the entire first exon, and a part of the first intron.

We have compared the previously described human *ATPase II* promoter [22] with putative *ATPase II* promoters found in several mammalian genomes (see Supplementary Fig. 1) We have found blocks of high homology or identity. These striking similarities are seen throughout the entire regions compared, and include putative promoters, 5′ UTRs, the coding region within the first exon as well as substantial portions of the 5′ end of intron 1. The comparison also revealed the presence of regions found only in one particular genome as well as regions found in two or more genomes.

Having identified the putative promoter region and the 5′UTR, we then analyzed the entire promoter region shown in Fig. 1A for the presence of a putative promoter as well as potential TF binding sites. PromoterInspector analysis of the putative promoter predicted the presence of a promoter from bp 889 to 1080 (Fig. 1A). Subsequent search for TF binding sites was carried out in two ways. We first determined the phylogenetic sequence conservation between mouse promoter described here along with the previously characterized human *ATPase II* promoter (variant I of the human promoter; AY775564, [22]) using DiAlingTF. Our analysis revealed the presence of nine clusters of transcription factor binding sites, which extended between bases -830 to +190 relative to the transcription start site (TSS) (Fig. 1A). Detailed analysis of each of these clusters revealed that they contain either a single (e.g. cluster -830/-814), a few (e.g. cluster -645/-625), or multiple (e.g. cluster -101/+6) potential TF binding sites conserved between the mouse and the human *ATPase II* promoters (Fig. 1B). Subsequently we analyzed the mouse promoter for the presence of all potential TF binding sites using MatInspector [34] which revealed the presence of densely packed potential TF binding sites within the entire putative mouse *ATPase II* promoter. The phylogenetically conserved TF binding sites are shown in Fig. 1B, whereas the other potential binding sites have been listed in Supplementary Table I. A large number of bindings sites for zinc-finger containing TFs have been predicted in the immediate vicinity and within the region detected by PromoterInspector as a potential mammalian promoter.

Taken together, our initial observations strongly suggested the presence of the mouse *ATPase II* promoter within the region immediately upstream of the coding sequence. In order to prove our hypothesis, we designed primers ATPaseFORW and ATPaseRev (Table I) and PCR amplified the putative *ATPase II* promoter from mouse genomic DNA. The amplification resulted in a single product of the approximate size of 1.2 kb, which upon sequencing was found to be nearly 100% identical (except for a single G-A substitution) to the same region found in Unfinished High Throughput Genomic Sequences (htgs) clones in the mouse genome

(Fig. 1A). In our investigations we have referred to this clone (-1026/+193 relative to the TSS identified by the 5′RACE studies presented in section 3.3) as “full promoter”.

3.2. Analysis of the activity of three segments of the 1.2-kb flanking region of the mouse ATPaseII gene

Our initial studies have focused on the dissection of mouse *ATPase II* full promoter into two regions, one immediately upstream of the translation start site, dubbed as “core promoter” (-318/+193 relative to the TSS), and including the putative promoter predicted by PromoterInspector. The remaining upstream segment was named as “distal promoter” (-1026/-299 relative to the TSS) (Fig. 1A).

We then tested transcriptional activities of each segment (Fig. 2) and found that in each cell line investigated, the activity of the core promoter was the highest followed by the activity of the full promoter. In general, the full promoter appeared to be almost equally active in neural and non-neural cells and the activity of the distal promoter was always the lowest of the three tested. In fact, statistical analysis revealed that in all cell lines transcriptional activity of the distal promoter was not significantly different from that of the empty vector (pGL3-Basic). For this reason no further studies were carried out on the distal promoter.

3.3. Identification of tissue type-dependent transcription-start sites

The transcription start site of the mouse *ATPase II* gene has not yet been identified. Additionally, the predicted *ATPase II* promoter sequence is devoid of a TATA box or a consensus eukaryotic initiator sequence. As observed earlier with the human *ATPase II* promoter, such TATA-less promoters often contain multiple transcription start sites [22]. We used RLM-RACE to determine transcription start sites in the mouse *ATPase II* promoter in four tissue types. As mentioned earlier, this technique precludes the inclusion of truncated products from reverse transcription that do not have a 5′-cap. Secondary products were clearly visible upon analysis by agarose gel electrophoresis (Fig. 3 panels A and B). Major single-size products, approximately 350-bp, were amplified from cDNAs obtained from heart, lung, and spleen. In addition, RLM-RACE of heart and spleen mRNA gave two shorter species of approximately 150 and 230-bp respectively. Sequence analysis of the 5′-RACE products revealed the presence of 5′ UTRs (upstream of the translation start site) of the sizes equal to 220 bp, 158 bp, 224 bp and 221 bp from spleen, heart, lung and liver respectively. The transcription start sites were confirmed from at least two independently isolated clones for each tissue type and in each case, the multiple clones analyzed from each tissue type yielded identical results. The 5′UTRs were almost identical in sequence (Fig. 3, panel C) in the regions where they overlap with a few single base substitutions. We have subsequently compared the 5′ ends of our RACE clones with the 5′ ends of ATPase II cDNA clones reported by others. This allowed us to identify additional TSS within the promoter of the *ATPase II* gene (Fig. 3C). This analysis revealed that transcription is initiated from two regions within the promoter located approximately 200-200-bp and approximately 152-162-bp upstream of the translation start site, respectively.

Our previous studies on TATA less promoters have revealed the presence of single nucleotide changes in 5′UTRs obtained from different sources or between 5′UTRs [22,42,43]. Similarly, we found only a few differences in the sequence of the promoter from the mouse genome sequence reported so far. We have subsequently compared the sequences of the 5′ RACE products to the sequence of genomic DNA. The product with the longest 5′ UTR was obtained from lung cDNA. Exact comparison of the cDNA sequence with the sequence of the gDNA from which the product had been transcribed revealed that the first two bases of the cDNA did not match with the genomic DNA sequence. Detailed analysis of the ATPase II clones available from public databases revealed the presence of eight clones where such mismatches were found

usually between the first base of cDNA and the corresponding base within gDNA (Supplementary Table II).

3.4 Deletion analysis of the core promoter

We have established that the core promoter region showed the strongest transcriptional activity, followed by transcriptional activity of the "full promoter" and very low or no activity shown by the "distal promoter". Analysis of the full promoter with PromoterInspector also predicted the presence of a potential promoter within the core region densely packed with potential TF binding sites. Moreover, our 5′ RACE as well as data obtained from analysis of ATPase II clones available from public databases place transcription start sites within the core promoter.

To further characterize the transcriptional activity of the core promoter, we adopted the classical approach of generating deletion mutants of the core promoter and testing their transcriptional activities (Fig. 4). The activity of the full promoter (-1026/+193) was always significantly lower than that of the -318/+193 mutant (core promoter) ($P < 0.0001$), although with B16F10 the P value was on the borderline of significance (0.054). Among the promoter fragments, the core promoter (-318/+193) showed the highest transcriptional activity in N18 and B16F10 cells, whereas a further deletion of 48 bp (-270/+193) resulted in a significant drop in activity in the N18 cells ($P <0.0001$) and a trend of decrease in the B16F10 ($P = 0.13$). Subsequent removal of 52 bp (-218/+193) caused a further decrease in activity in N18 cells ($P <0.0001$) but not in B16F10. By contrast, in all the remaining cell lines, no such attenuation below the activity of the core promoter was observed in these fragments. In SN48 cells there were no statistically significant differences detected between transcriptional activities of the core promoter and the deletion fragments -270/+193 or -218/+193. In HN2 as well as NIH3T3 cells, deletion of the first 48 bases (-270/+193) resulted in a significant increase in transcriptional activity ($P<0.002$) although further deletions (-218/+193) did not result in any further increase in the HN2 cell line ($P<0.02$) and, in fact, caused a decrease in activity in the NIH3T3 cell line ($P <0.0001$). Further deletion to -172/+193 caused a significant decrease in activity only in HN2 cells ($P =0.0001$). Upon further deletion of the promoter to -119, a significant decrease in transcriptional activity was observed in all cell lines ($P <0.0001$).

All deletion mutants including the -172/+193 still retained the entire putative promoter region predicted by PromoterInspector (on Fig. 1A, -158/+54 relative to the TSS). Therefore it was not surprising that almost all of them retained almost full transcriptional activity. Further deletions to -119, resulted in a significant loss of transcriptional activity in all cells ($P <0.04$). Similarly, in all cells, deletion to -70 and beyond resulted in a very sharp loss of transcriptional activity as compared to that of the core promoter. In B16F10 and in NIH3T3 cells, there were no significant differences between activities of the -70 mutant and the activities of -119/+193 ($P=1$). Subsequent deletions to -13 resulted in a further sharp decrease in activity in all cell lines. In all cells tested, further deletions from -13 to +33 had no effect. With the exception of SN48 cells, the minimum activity of the deleted promoter (+33/+193) was not significantly higher than that of the empty vector.

We have also cloned the core promoter into antisense orientation with respect to the luciferase reporter gene (construct +193/-318) and tested luciferase activity of the construct obtained. A strong activity was observed in all cells tested and showed a trend of being even higher than that of the core promoter in the NIH3T3 cells ($P=0.07$), and higher than that of the full promoter (-1026/+193) in NIH3T3, SN48 and HN2 cells. In order to further understand the mechanism driving expression from the core promoter in antisense orientation, we have analyzed the sequence of the complementary strand of the full promoter for the presence of potential mammalian promoters using PromoterInspector. The presence of a promoter was predicted between bases 121 and 348 on the complementary strand. In Fig. 1A (original strand) this would correspond to bases 1099-872. Moreover, the presence of the mammalian C-type LTR

TATA box has been predicted between bases 783 and 799 (–244/–288 relative to the TSS) on the negative strand (Fig. 1A and Supplementary Table I). The presence of these predicted features has therefore prompted us to explore the possibility that the *ATPase II* promoter harbors bidirectional activity *in vivo*. We searched public databases using the "full promoter" sequence as a query for the presence of messages showing a plus/minus match and a nearly 100% identity over a significant part of the full promoter. Finding such messages would bring in the possibility that they had been transcribed from the *ATPase II* promoter but in an orientation reverse to that of the ATPase II message. So far we have found no such messages.

3.5. Determination of the mouse ATPase II gene structure

Having identified the *ATPase II* promoter and determined the transcription start sites, we then decided to delineate the organization of the entire mouse *ATPase II* gene. Comparative analysis and critical review of cDNA sequences available as well as drafts of mouse genome was carried out as described previously [22,42,43]. Data presented in this paper were obtained using NCBI Reference Sequences (RefSeq) NM_009727 and NM_001038999 as well as most recent mouse genome draft freeze of February 2006. The exon/intron organization of *ATPase II* gene is outlined in Fig. 5B (for further details see Supplementary Table III). The *ATPase II* gene has been mapped to the negative strand of chromosome 5, region qC3.1, and extends between bases 68,126,566 and 67,901,831 (224,735 bp). The coding region of the *ATPase II* consists of 38 exons, varying in size between 41 bp (exon 6) to >4557 bp (exon 38). Two splice variants of ATPase II cDNA have been reported in public database, the RefSeq NM_001038999.1 (GI: 84781801) and NM_009727.2 (GI:84781809). The former, contains exons 1-6 and 8-38 is referred to as a transcript variant 1 and gives rise to the protein of 1164 amino acids (isoform a). The latter, containing exons 1-7, 9-15 and 17-38 is referred to as a transcript variant 2 and gives rise to the protein of 1149 amino acids (isoform b).

Subsequent analysis of mouse ATPase II cDNA clones of sufficient size available from public databases revealed that alternative splicing of exons 7 and 8 as well as co-occurrence of exons 8 and 16 is a rule among all the clones examined. In particular we found exon 7 in clones NM_009727.2, U75321.1, AK076388.1 and exons 8 and 16 in clones NM_001038999.1, AK220560.1, AK141559.1, AK045367.1. No other transcript variants with respect to exons 7, 8 and 16 were found among ATPase II clones of sufficient size.

Sequences of mouse ATPase II protein isoforms a and b are shown in Supplementary Figure 2A. We observed a salient difference between these two isoforms, which was in a stretch of 16 amino acids. While isoform a of ATPase II contained these amino acids, they were absent from the isoform b in all species. A further sequence variation was that exons 7 and 8 were alternatively used in isoforms a and b, respectively. Interestingly, a stretch of 24 amino acids, which is different between the two isoforms, is encoded by the alternatively used exons 7 and 8, respectively.

Cross-species comparison of ATPase II protein sequences from databases was completed next. We have compared sequences from human, murine, bovine and canine genomes and have found a very high degree of homology across species (data not shown here). Interestingly, the size of either isoform a or isoform b remained exactly the same across all species considered here. This shows that the sequence variations resulting from alternative splicing was exactly the same as that observed in the mouse isoforms (Supplementary Figure 2B).

The last exon encodes the 3′ end of the *ATPase II* transcript including the STOP codon and a long 3′ UTR. In fact, the untranslated region accounts for 4459 bp, which is more than half of the entire cDNA for either transcript variant. No repetitive elements have been located in the 3′UTR (data not shown here). Analysis of the sequence of the 3′UTR for the presence of polyadenylation signals revealed the presence of four AAUAAA (e.g. in RefSeq NM_09727.2

bases 6133-6138, 7087-7092 and 8103-8108, 8108-8113 which is: 2462, 3416, 4432 and 4437 bp downstream of the stop codon, respectively) and five AUUAAA signal sequences (e.g. in RefSeq NM_09727.2 bases 5293-5298, 6537-6542, 7082-7087, 7148-7153 and 8096-8101, which is: 1622, 2866, 3411, 3477 and 4425 bp downstream of the stop codon, respectively) (not shown).

4. Discussion

Multiple members of the superfamily of P-type ATPases have been described in the literature and the coding sequences and expression profiles of many of these proteins have been identified. However, to date, the promoter regions and 5′UTRs of only few P-type ATPases have been characterized. These include the promoter and 5′UTR of mouse *ATPase II* gene reported here, the human counterparts reported by our group earlier [22], and the promoter region of the Wilson Disease Gene (WDG) [23,44]. All the promoters characterized so far lack TATA boxes and contain GC-rich regions harboring multiple TF binding sites. For the human *ATPase II* promoter we have cloned and characterized two variants differing from each other by the absence or presence of a 15-bp direct repeat immediately upstream of the transcription start site [22]. By contrast, our current analysis of mouse *ATPase II* promoter clones, which were independently amplified and analyzed has revealed only one version of the mouse promoter. Also, no other promoter variants have been reported in murine databases and literature.

Multiple transcription start sites have been identified within CpG islands on both human [22] and mouse *ATPase II* genes (Fig. 3A and Supplementary Table II). In contrast to the mouse *ATPase II* gene, a single transcription start site was identified in the promoter of the WDG [44], but this site was also within a GC-rich region. It is tempting to speculate that the expression from each of the three P-type *ATPase II* promoters described is driven by G-rich binding, triple zinc-finger family of TFs [45,46].

Initial deletion analysis of the promoter (Fig. 2) indicated that transcriptional activity of the distal promoter was much lower than that of the full or core promoter fragments and was statistically undistinguishable from that of the empty reporter vector in all cell lines tested. Subsequent studies on transcriptional activity of the deletion mutants (Fig. 4) revealed that in all cell lines except B16F10, the core promoter displayed significantly higher activity than the full promoter. In HN2 and NIH3T3 cells the transcriptional activity was further increased after deletion of the 5′ end (construct -270/+193 vs. core) but not in the remaining cell lines. This suggests that depending on cell types, the TF binding sites could be utilized differentially. PromoterInspector predicted the presence of the promoter within bases 868-1080 (-159/+54 relative to the TSS). In all cell lines, the presence of this region (mutant -172/+193) was sufficient for high transcriptional activity of the deletion mutant, sometimes even higher than that of the full or core promoter. However, 5′ serial deletions eventually resulted in a sharp decrease of the promoter activity when portions of the predicted promoter were removed. Complete elimination of the promoter activity in all cells was observed upon deletion from -70 to -13, which strongly suggests that the minimal essential promoter is located within the region of -13 to -70 relative to the TSS. Taken together, this suggests that the essential promoter region is most likely located more or less exactly within the region predicted by the PromoterInspector.

Furthermore, our data demonstrated relatively little tissue specificity of the mouse *ATPase II* promoter. This finding is agreement with our previously published data on the human *ATPase II* promoter [22]. However, tissue specific expression of ATPase II mRNA has been reported [14,21]. Therefore, if ATPase II expression is regulated at the level of transcription, the elements responsible for its tissue specific expression must be located either in the region(s) further upstream of the full promoter region or perhaps within the large first intron.

Analysis of the structure of *ATPase II* gene has revealed the presence of 38 exons, which upon alternative splicing involving exons 7, 8 and 16 give rise to two transcription variants that in turn results in two forms of ATPase II proteins containing 1149 and 1164 amino acids, respectively. Human ATPase II proteins of the same sizes have been reported earlier, with the tissue specific expression of the alternatively spliced message coding for the two proteins [14]. In contrast to mouse ATPase II, the alternative splicing of human ATPase II messages reported in the literature [14,22] only involved either inclusion or exclusion of the human counterpart of mouse exon 16 (Supplementary Table III). Ding and coworkers have reported two forms of bovine ATPase II proteins that differ in the absence or presence of a 15-amino acid insert encoded by exon 16 [13].

Unfortunately, no information could be obtained on tissue specificity of the two mouse transcript variants. The 5′RACE products reported here may in fact represent either or both variants in each tissue because the primers used for the 5′RACE were selected from the exons that were present in either transcript variants and were therefore not alternatively spliced. As far as genomic organization is concerned, both mouse *ATPase II* and its human counterpart [22] are similar in structure. The human *ATPase II* gene consists of 37 exons, and with the exception of the first (5′ UTR and 5′end including the translation start site) as well as the last (3′end, STOP codon and 3′UTR) exons, the sizes of murine and human exon counterparts are exactly the same. The transcription start site in the human *ATPase II* gene is located only 150-bp from the translation start site [22], resulting in a much shorter 5′UTR than its murine counterpart reported here. Since our last publication on the human *ATPase II* [22] new human ATPase II cDNA clones have been reported. Comparison of sequences of these clones with the sequence of the human *ATPase II* gene indicates that transcription of these clones start within the region located approximately 200-240 bp from the translation start site, which is further upstream to the TSSs reported by us earlier. Also, mouse ATPase II cDNAs with shorter 5′UTRs have been reported in public databases (Fig. 3c, Supplementary Table II). Thus, there is considerable similarity between mouse and human promoters in the position of transcriptional initiation. The tissue specificity and conditions under which transcription starts from different regions within *ATPase II* promoter will be investigated in our future projects.

The last exon in the mouse *ATPase II* gene is much longer than all the remaining exons and encodes a long 3′UTR. In our previous studies on the human F11 receptor/junctional adhesion molecule 1 [42,43], we had used 3′ RACE along with information from public databases to explain the existence of mRNAs differing at their 3′ends and suggested the possible function of the two polyadenylation signal found in the 3′ UTR of the F11R message. The 3′UTR for the mouse ATPase II message (RefSegs: NM_001038999.1 (GI:84781801) and NM_009727.2 (GI:84781809) contains multiple potential polyadenylation signals. In the case of human ATPase II, a single message of approximately 9.5 kb was detected by the Northern blotting, which is somewhat in agreement with the sizes of mATPase II RefSeqs (8175 and 8130-bp, respectively). However, no information is available on the size of the mouse ATPase II message. The cDNA clone BC094235, the only one with an experimentally established 3′-end is incomplete at its 5′-end, including the beginning of the coding sequence. This clone terminates after the first pair of closely spaced/partially overlapping ATTAAA/AATAAA located 3410 bp and 3415 bp downstream, respectively, of the stop codon. It is conceivable that the clones with long 3′-end terminate after the second pair of closely spaced AATAAA and ATTAAA polyadenylation signal sequences located 4432, 4425 and 4437 bp downstream of the stop codon. However, this is only the case with the RefSeqs and has not been reported with any other full length mouse ATPase II cDNA clones. In human ATPase II cDNA clone AB209687.1 (GI:62088953) two closely spaced signal sequences ‘ATTAAA’ followed by a ‘AATAAA’ are located 4509 and 4520 bp respectively downstream of the stop codon, a striking similarity to the mouse RefSeq clones. Future studies, which are beyond the purview of this article, will address such issues since the size of 3′ UTR determines stability of the messages.

While we found no literature evidence for bidirectional transcriptional activity of the *ATPase II* promoter described here, further studies will address this issue. Bidirectional (divergent) gene configuration has been shown to occur frequently in the human genome representing more than 10% of genes and described especially in DNA repair genes, non-DNA repair nuclear process genes and genes encoding metabolic pathway proteins. Bidirectional gene arrangement has been shown to be conserved among mouse homologs [47,48]. Moreover, the presence of CpG islands [41] has been demonstrated within the loci where two genes overlap in their divergent (head-to-head) orientation [47]. Some human endogenous retrovirus insertions long terminal repeats are known to contain bidirectional activities in reporter gene assays. The transcription of two genes *DSCR4* and *DSCR8* have been demonstrated to originate from shared ERV LTR bidirectional promoter ([49] and literature cited therein). Analysis of public databases revealed the presence of two clones AK035785 and AK044198 that originate from closely spaced sites in mouse genome and correspond to intron 1 of the *ATPase II* gene. Transcription of the clones begins 97 bp, AK035785 and 27bp, AK044198 upstream of exon I/intron I junction in the *ATPase II* gene and the clones are transcribed on the plus strand of mouse chromosome 5, while *ATPase II* gene has been located in the minus strand. Putative genes for AK035785 and AK044198 contain four and three exons respectively. The sequences of the clones encoded by part of their exon 1 match to bases 208 to 275 (plus/minus match) of our longest 5′ RACE clone (lung, DQ503477.1; GI:95116731).

P-type ATPases have been shown to be essential for cell functioning. Consequently this protein and its homologs have received much attention in recent years. Their involvement in multiple drug resistance, Wilson's disease, and familial Cholestasis has been established in earlier studies [5,24,50].

Our previous studies have shown that apoptosis is associated with an inhibition of APTL and externalization of PS [7,10]. We have also demonstrated that overexpression of ATPase II in the hybrid neuroblastoma cell line HN2 causes an increase in APTL activity [17], which suggests the possibility that ATPase II is indeed involved in PS translocation. During apoptosis, many other genes and their products are regulated to cause signature changes that are observed in the apoptotic cells. Collectively, it calls for extensive investigation of ATPase II expression in various cell types under different conditions of trophic support or stress. Results of the studies on ATPase II gene presented here as well as reported by our group earlier [22,51] lay the groundwork for such future experiments, which will help delineate the role of ATPase II.

Supplementary Material

Refer to Web version on PubMed Central for supplementary material.

Glossary

Abbreviations:

APTL, aminophospholipid translocase; ATF, Activating transcription factor; gDNA, genomic DNA; HGP, Human Genome Project; htgs, Unfinished High Throughput Genomic Sequences: phases 0, 1 and 2; NCBI, National Center for Biotechnology Information; RefSeq, NCBI Reference Sequence (see: http://ncbi.nih.gov/RefSeq/); RLM-RACE, RNA ligase-mediated rapid amplification of cDNA ends; SP, Stimulating protein 1 ubiquitous zinc finger transcription factor; TF, transcription Factor; TSS, transcription start site; USF, Upstream stimulating factor; WDG, Wilson Disease Gene.

References

[1]. Zwaal RFA, Schroit AJ. Pathophysiologic implications of membrane phospholipid asymmetry in blood cells. Blood 1997;89:1121–1132. [PubMed: 9028933]

[2]. Daleke DL. Regulation of transbilayer plasma membrane phospholipid asymmetry. J. Lipid Res 2003;44:233–242. [PubMed: 12576505]

[3]. Daleke DL, Lyles JV. Identification and purification of aminophospholipid flippases. Biochimica et Biophysica Acta (BBA) - Molecular and Cell Biology of Lipids 2000;1486:108–127.

[4]. Raggers RJ, Pomorski T, Holthuis JCM, Kalin N, van Meer G. Lipid Traffic: The ABC of Transbilayer Movement. Traffic 2000;1:226–234. [PubMed: 11208106]

[5]. Choi C-H. ABC transporters as multidrug resistance mechanisms and the development of chemosensitizers for their reversal. Cancer Cell International 2005;5

[6]. Schlegel RA, Williamson P. Phosphatidylserine, a death knell. Cell Death and Differentiation 2001;8:551–536. [PubMed: 11536005]

[7]. Adayev T, Estephan R, Meserole S, Mazza B, Yurkow EJ, Banerjee P. Externalization of phosphatidylserine may not be an early signal of apoptosis in neuronal cells, but only the phosphatidylserine-displaying apoptotic cells are phagocytosed by microglia. Journal of Neurochemistry 1998;71:1854–1864. [PubMed: 9798909]

[8]. Fadok VA, Voelker DR, Campbell PA, Cohen JJ, Bratton DL, Henson PM. Exposure of phosphatidylserine on the surface of apoptotic lymphocytes triggers specific recognition and removal by macrophages. Journal Of Immunology (Baltimore, Md.: 1950) 1992;148:2207–2216. [PubMed: 1545126]

[9]. Verhoven B, Krahling S, Schiegel RA, Williamson P. Regulation of phosphatidylserine exposure and phagocytosis of apoptotic T lymphocytes. Cell Death and Differentiation 1999;6:262–270. [PubMed: 10200577]

[10]. Das P, Estephan R, Banerjee P. Apoptosis is associated with an inhibition of aminophospholipid translocase (APTL) in CNS-derived HN2-5 and HOG cells and phosphatidylserine is a recognition molecule in microglial uptake of the apoptotic HN2-5 cells. Life Sciences 2003;72:2617–2627. [PubMed: 12672507]

[11]. Tang X, Williamson P, Halleck MS, Schlegel RA. A subfamily of P-type ATPases with aminophospholipid transporting activity. Science 1996;272:1495–1497. [PubMed: 8633245]

[12]. Bitbol M, Fellmann P, Zachowski A, Devaux PF. Ion regulation of phosphatidylserine and phosphatidylethanolamine outside-inside translocation in human erythrocytes. Biochimica et Biophysica Acta - Biomembranes 1987;904:268–282. [PubMed: 3117114]

[13]. Ding J, Wu Z, Crider BP, Ma Y, Li X, Slaughter C, Gong L, Xie X-S. Identification and Functional Expression of Four Isoforms of ATPase II, the Putative Aminophospholipid Translocase. EFFECT OF ISOFORM VARIATION ON THE ATPase ACTIVITY AND PHOSPHOLIPID SPECIFICITY. J. Biol. Chem 2000;275:23378–23386. [PubMed: 10801890]

[14]. Mouro I, Cartron J-P, Colin Y, Halleck MS, Schlegel RA, Mattei MG, Williamson P, Zachowski A, Devaux P. Cloning, expression, and chromosomal mapping of a human ATPase II gene, member of the third subfamily of P-type ATPases and orthologous to the presumed bovine and murine aminophospholipid translocase. Biochemical and Biophysical Research Communications 1999;257:333–339. [PubMed: 10198212]

[15]. Pomorski T, Lombardi R, Riezman H, Devaux PF, van Meer G, Holthuis JCM. Drs2p-related P-type ATPases Dnf1p and Dnf2p Are Required for Phospholipid Translocation across the Yeast Plasma Membrane and Serve a Role in Endocytosis. Mol. Biol. Cell 2003;14:1240–1254. [PubMed: 12631737]

[16]. Halleck MS, Pradhan D, Blackman C, Berkes C, Williamson P, Schlegel RA. Multiple members of a third subfamily of P-type ATPases identified by genomic sequences and ESTs. Genome Research 1998;8:354–361. [PubMed: 9548971]

[17]. Chin G, El-Sherif Y, Jayman F, Estephan R, Wieraszko A, Banerjee P. Appearance of voltage-gated calcium channels following overexpression of ATPase II cDNA in neuronal HN2 cells. Molecular Brain Research 2003;117:109–115. [PubMed: 14559144]

[18]. Jayman, F. Functional And Structural Analysis Of The Mouse ATPase II Gene. Graduate Center, City University of New York; New York, NY: 2006.

[19]. Kuhlbrandt W. Biology, Sructure and Mechanism Of P-Type ATPases. Nature Reviews Molecular Cell Biology 2004;5:282–295.

[20]. Paulusma CC, Oude RPJ. Elferink, The type 4 subfamily of P-type ATPases, putative aminophospholipid translocases with a role in human disease. Biochimica et Biophysica Acta (BBA) - Molecular Basis of Disease 2005;1741:11–24. [PubMed: 15919184]

[21]. Halleck MS, Lawler JF JR, Blackshaw S, Gao L, Nagarajan P, Hacker C, Pyle S, Newman JT, Nakanishi Y, Ando H, Weinstock D, Williamson P, Schlegel RA. Differential expression of putative transbilayer amphipath transporters. Physiol. Genomics 1999;1:139–150. [PubMed: 11015572]

[22]. Sobocki T, Jayman F, Sobocka MB, Duchatellier R, Banerjee P. Isolation, sequencing, and functional analysis of the TATA-less human ATPase II promoter. Biochimica et Biophysica Acta (BBA) - Gene Structure and Expression 2005;1728:186–198. [PubMed: 15833447]

[23]. Cullen LM, Prat L, Cox DW. Genetic variation in the promoter and 5′ UTR of the copper transporter, ATP7B, in patients with Wilson disease. Clinical Genetics 2003;64:429–432. [PubMed: 14616767]

[24]. Bull PC, Thomas GR, Rommens JM, Forbes JR, Cox DW. The Wilson disease gene is a putative copper transporting P-type ATPase similar to the Menkes gene. Nat Genet 1993;5:327–337. [PubMed: 8298639]

[25]. Tanzi RE, Petrukhin K, Chernov I, Pellequer JL, Wasco W, Ross B, Romano DM, Parano E, Pavone L, Brzustowicz LM, Devoto M, Peppercorn J, Bush AI, Sternlieb I, Pirastu M, Gusella JF, Evgrafov O, Penchaszadeh GK, Honig B, Edelman IS, Soares MB, Scheinberg IH, Gilliam TC. The Wilson disease gene is a copper transporting ATPase with homology to the Menkes disease gene. Nat Genet 1993;5:344–350. [PubMed: 8298641]

[26]. Vulpe C, Levinson B, Whitney S, Packman S, Gitschier J. Isolation of a candidate gene for Menkes disease and evidence that it encodes a copper-transporting ATPase. Nat Genet 1993;3:7–13. [PubMed: 8490659]

[27]. Yamaguchi Y, Heiny ME, Gitlin JD. Isolation and Characterization of a Human Liver cDNA as a Candidate Gene for Wilson Disease. Biochemical and Biophysical Research Communications 1993;197:271–277. [PubMed: 8250934]

[28]. Consortium MGS. Initial sequencing and comparative analysis of the mouse genome. Nature 2002;420:520–562. [PubMed: 12466850]

[29]. Kent WJ. BLAT--the BLAST-like alignment tool. Genome Research 2002;12:656–664. [PubMed: 11932250]

[30]. Kent WJ, Sugnet CW, Furey TS, Roskin KM, Pringle TH, Zahler AM, Haussler D. The human genome browser at UCSC. Genome Research 2002;12:996–1006. [PubMed: 12045153]

[31]. Thompson JD, Higgins DG, Gibson TJ. CLUSTAL W: Improving the sensitivity of progressive multiple sequence alignment through sequence weighting, position-specific gap penalties and weight matrix choice. Nucleic Acids Research 1994;22:4673–4680. [PubMed: 7984417]

[32]. Smith RF, Wiese BA, Wojzynski MK, Worley KC, Davison DB. BCM search launcher - An integrated interface to molecular biology data base search and analysis services available on the World Wide Web. Genome Research 1996;6:454–462. [PubMed: 8743995]

[33]. Scherf M, Klingenhoff A, Werner T. Highly specific localization of promoter regions in large genomic sequences by PromoterInspector: A novel context analysis approach. Journal of Molecular Biology 2000;297:599–606. [PubMed: 10731414]

[34]. Cartharius K, Frech K, Grote K, Klocke B, Haltmeier M, Klingenhoff A, Frisch M, Bayerlein M, Werner T. MatInspector and beyond: promoter analysis based on transcription factor binding sites. Bioinformatics 2005;21:2933–2942. [PubMed: 15860560]

[35]. Morgenstern B, Dress A, Werner T. Multiple DNA and protein sequence alignment based on segment-to-segment†comparison. PNAS 1996;93:12098–12103. [PubMed: 8901539]

[36]. Morgenstern B, Frech K, Dress A, Werner T. DIALIGN: finding local similarities by multiple sequence alignment. Bioinformatics 1998;14:290–294. [PubMed: 9614273]

[37]. Morgenstern B. DIALIGN 2: improvement of the segment-to-segment approach to multiple sequence alignment. Bioinformatics 1999;15:211–218. [PubMed: 10222408]

[38]. Motulsky, H. Intuitive Biostatistics. Oxford University Press; 1995.

[39]. Altschul SF, Gish W, Miller W, Meyers EW, Lipman DJ. Basic Local Alignment Search Tool. Journal of Molecular Biology 1990;215:403–410. [PubMed: 2231712]

[40]. Schwartz S, Kent WJ, Smit A, Zhang Z, Baertsch R, Hardison RC, Haussler D, Miller W. Human-Mouse Alignments with BLASTZ. Genome Res 2003;13:103–107. [PubMed: 12529312]

[41]. Gardiner-Garden M, Frommer M. CpG islands in vertebrate genomes. Journal of Molecular Biology 1987;196:261–282. [PubMed: 3656447]

[42]. Sobocki T, Sobocka MB, Babinska A, Ehrlich YH, Banerjee P, Kornecki E. Genomic structure, organization and promoter analysis of the human F11R/F11 receptor/junctional adhesion molecule-1/JAM-A. Gene 2006;366:128–144. [PubMed: 16337094]

[43]. Sobocki, T. Genomic Organization of Human F11R/JAM and Identification of Two Types of mRNAs Regulated by Alternative Promoters. School of Graduate Studies, State University of New York, Downstate Medical Center; Brooklyn, NY: 2001.

[44]. Oh WJ, Kim EK, Park KD, Hahn SH, Yoo OJ. Cloning and Characterization of the Promoter Region of the Wilson Disease Gene. Biochemical and Biophysical Research Communications 1999;259:206–211. [PubMed: 10334941]

[45]. Philipsen S, Suske G. A tale of three fingers: the family of mammalian Sp/XKLF transcription factors. Nucl. Acids Res 1999;27:2991–3000. [PubMed: 10454592]

[46]. Suske G. The Sp-family of transcription factors. Gene 1999;238:291–300. [PubMed: 10570957]

[47]. Adachi N, Lieber MR. Bidirectional Gene Organization: A Common Architectural Feature of the Human Genome. Cell 2002;109:807–809. [PubMed: 12110178]

[48]. Trinklein ND, Aldred SF, Hartman SJ, Schroeder DI, Otillar RP, Myers RM. An Abundance of Bidirectional Promoters in the Human Genome. Genome Res 2004;14:62–66. [PubMed: 14707170]

[49]. Dunn CA, Romanish MT, Gutierrez LE, van de Lagemaat LN, Mager DL. Transcription of two human genes from a bidirectional endogenous retrovirus promoter. Gene 2006;366:335–342. [PubMed: 16288839]

[50]. Bull LN, Van Eijk MJT, Pawlikowska L, DeYoung JA, Juijn JA, Liao M, Klomp LWJ, Lomri N, Berger R, Scharschmidt BF, Knisely AS, Houwen RHJ, Freimer NB. A gene encoding a P-type ATPase mutated in two forms of hereditary cholestasis. Nature Genetics 1998;18:219–224. [PubMed: 9500542]

[51]. Sobocki, T.; Duchatellier, R.; Sobocka, MB.; Ray, I.; Banerjee, P. Isolation, Functional Analysis, And Cell Type Specificity Of The Human Aminophospholipid Translocase (APTL) II Promoter; 34th Annual Meeting of the American Society for Neurochemistry; Newport Beach, California. May 3-7, 2003;

A.

```
-1026/1    AAAGCCTTGC TACAGGCTCT TTCCGCTAGG TGCCCAGAAG AACAGTACAC GAAGCCAGTA CCTTTTACCT TTATTCCTTT CTTACCCTGC TCAGGAGCTT GCTAGACACA AAGCTCCCCT
 -906/121  CATCCTATCT CGAGGCTGAA ATCGGGAACA AATTAAAAAT ACTGCATTTG TTTCGACTTG TTAGATTGGA TTTTACTACA CAAAATAAAA GGCACTGAGG TCGTGCTGGT CTCTAGGACA
 -786/241  TAACGACTTG TAATTAACAT CTTTATGGAT TTTATACCGA CGCCCCACTA GGCTTTGAGG ATAAACTACT GCATCGAACT TTCTGGAGCA GAAACCACAA ACAGCATAAT TTTTGCTTGG
 -666/361  TTAACCACGT GGTCAACAGT TGGTTTGGTT GCAGTTTCAG AGCCTTAACA GGTTGCAGAG GACGAACTGG TGGGAAGTAC GGACTCACAC ACCCACGCAG GTTGTGTGGC TGGAAGCCTT
 -546/481  AAAACGACAA GAGGAACCGT TCCAGTGGCT TCAGGTCTCA CAGCCTGCTA CTACAGAGGG TTCACGTTCA TCTCAGGCCA GGAGTCAGGC TGGGTGTTGA GATAGGCTAG GATTCCACTC
 -426/601  AGAGGGCGAA TGCAGGGTCC CCCCACATCA GCAGAGACGT CACCCACAGA GTCTCAGAGG CTTAGACTCA AGCTGCCCAC ACCGAACCCA ACACCCTGGC GCTGAGGACG GTCGGTTCTA
 -306/721  TCGCATTGTA GAGCCAGAAG GTGGCTGTAG GGGATGCCAG AGCTTTCAGA GCTAAAGAAG CTCTTCCTCT TTTATTAAGG CTTGGGACAC TTGTACTGGC CTCAAGGAGG GCCGAGGTGG
 -186/841  GCCGAGAAGC CGAGAATGCT AGATCGAAGT CCCCTCCCCG CGGATGGTAC GGTCCGAACT GGGCGGGACC TGGAGGCTCG GCGGCCCTGT CCCCGCCCCA CTCCAGGAGG CCAGCGAGTG
  -66/961  AGCGCGCGCC CCGCAGACCC CGCCCCCGGC GCCGTCCCCG GCTCCGCCCC TCGAGCCCGC TCCTCTGCCA CTGCGGGGAG ACCTAGGCGG CTCTGCGGAC GCAGCTCCTT CGCCGCCTTC
  +55/1081 CCCCTCCCGT CCAGTGCCCA GGCGGCTCCT GGCGGCGACG CTGCCCTGGG TGGGAGGCGC GGCCCCGCGG CAGCTGAGCC CTCTGCGCGG CGCAGCCAGC TCTCCCGCCC GCGCGGCGCC
 +175/1201 GTGACAGGTG CAGGGTCCC 1219
```

B.

Matrix Name:	Transcription Factor	Str.	Position
V$EVI1.06	Ecotropic viral integration site 1 encoded factor, amino-terminal zinc finger domain	(+)	-830/-814
V$OCT1.06	Octamer-binding factor 1	(-)	-778/-764
V$MEIS1B_ HOXA9.01	Meis1b and Hoxa9 form heterodimeric binding complexes on target DNA	(+)	-772/-758
V$CLOX.01	Cut-like homeo box	(-)	-767/-749
V$CDP.02	Transcriptional repressor CDP	(-)	-767/-749
V$HNF6.01	Liver enriched Cut - Homeodomain transcription factor HNF6 (ONECUT)	(-)	-766/-750
V$OC2.01	CUT-homeodomain transcription factor Onecut-2	(-)	-766/-750
V$MYT1.02	MyT1 zinc finger transcription factor involved in primary neurogenesis	(-)	-715/-703
V$IRF3.01	Interferon regulatory factor 3 (IRF-3)	(-)	-645/-625
V$MOK2.01	Ribonucleoprotein associated zinc finger protein MOK-2 (mouse)	(+)	-637/-617
V$MZF1.02	Myeloid zinc finger protein MZF1	(+)	-279/-271
V$ZF9.01	Core promoter-binding protein (CPBP) with 3 Krueppel-type zinc fingers	(+)	-101/-79
V$SP1.01	Stimulating protein 1, ubiquitous zinc finger transcription factor	(-)	-99/-85
V$GC.01	GC box elements	(-)	-99/-85

Matrix Name:	Transcription Factor	Str.	Position
V$SP1.02	Stimulating protein 1, ubiquitous zinc finger transcription factor	(-)	-99/-85
V$KKLF.01	Kidney-enriched kruppel-like factor, KLF15	(-)	-98/-82
V$NRF1.01	Nuclear respiratory factor 1 (NRF1), bZIP transcription factor that acts on nuclear genes encoding mitochondrial proteins	(-) (+) (+)	-71/-55 -70/-54 -68/-52
V$ZF5.01	Zinc finger / POZ domain transcription factor	(+)	-69/-58
V$ZF9.01	Core promoter-binding protein (CPBP) with 3 Krueppel-type zinc fingers	(+) (+)	-54/-32 -17/+6
V$ZBP89.01	Zinc finger transcription factor ZBP-89	(+)	-54/-32
V$SP1.01	Stimulating protein 1, ubiquitous zinc finger transcription factor	(-) (-)	-52/-38 -28/-14
V$GC.01	GC box elements	(-) (-)	-52/-38 -28/-14
V$SP1.02	Stimulating protein 1, ubiquitous zinc finger transcription factor	(-) (-)	-52/-38
V$ZNF219.01	Kruppel-like zinc finger protein 219	(+)	-51/-29
V$ZF9.01	Core promoter-binding protein (CPBP) with 3 Krueppel-type zinc fingers	(+)	-30/-8
V$SP1.01	Stimulating protein 1, ubiquitous zinc finger transcription factor	(-)	-28/-14

Matrix Name:	Transcription Factor	Str.	Position
V$MAZ.01	Myc associated zinc finger protein (MAZ)	(-)	-23/-11
V$HEN1.02	HEN1 (E-box binding factor)	(-)	+117/+136
V$HEN1.01	HEN1 (E-box binding factor)	(-)	+117/+136
V$MEIS1.01	Binding site for monomeric Meis1 homeodomain protein	(-)	+173/+183
V$TAL1_ E2A.01	Complex of Lmo2 bound to Tal-1, E2A proteins, and GATA-1, half-site 1	(+)	+174/+190
V$MYOD.01	Myogenic regulatory factor MyoD (myf3)	(+)	+174/+190
V$MYOGENIN.01	Myogenic bHLH protein myogenin (myf4)	(+)	+174/+190
V$MEIS1A_ HOXA9.01	Meis1a and Hoxa9 form heterodimeric binding complexes on target DNA	(+)	+176/+190
V$AREB6.03	AREB6 (Atp1a1 regulatory element binding factor 6)	(-)	+176/+188
V$.MEIS1B_ HOXA9.01	Meis1b and Hoxa9 form heterodimeric binding complexes on target DNA	(+)	+176/+190

Figure 1.

Isolation and characterization of the mouse *ATPase II* promoter. TF binding sites predicted by DiAlign TF [35-37] conserved between mouse and human (AY775564, [22]) *ATPase II* promoters and present in regions where the sequences of the two promoters align. Panel A: Sequence of the mouse *ATPase II* promoter characterized in the present studies. For the purpose of simplicity double base numbering system is utilized on the left of each line. The base number is written (in boldface) relative to the transcription start site (section 3.3, Fig. 3) followed by (in regular typeface) consecutive base number starting from the 5′end of the sequence. The entire promoter sequence (bp 1-1219 or -1026/+193 relative to TSS) has been deposited into Genbank (Accession number DQ503476) and in section 3.1 is referred to as a ‘full promoter’. Deletion fragment, bp 1 to -299 (-1026/-299 relative to the TSS) has been named as ’distal promoter’ and fragment bp 709-1219 (-318/+193 relative to the TSS) has been termed as ‘core promoter’. The start of transcription is indicated by a symbol(). An asterisk (*) above the sequence indicates a base different from the mouse genome draft (freeze of February 2006). The mammalian promoter predicted by PromoterInspector (bases 869-1080, i.e. -158/+54 relative to the TSS) is underlined below the sequence. Alignment of the full promoter sequence to the coding sequence of the mouse ATPase II (for example to the NCBI RefSeq NM_009727.2, GI:84781809) indicates that the translation start site (ATG) is at +225 relative to the TSS. The 5′ part of the CpG island identified within the *ATPase II* gene covers bases

833 to 1219 and the island extends beyond the promoter region through the entire 5′UTR, the coding sequence and a part of the first exon. The white diamond line below the sequence (⟵)indicates the position of the Mammalian C-type LTR TATA box (on the negative strand), the presence of which may explain the activity of the core promoter placed in an antisense orientation with respect to the luciferase reporter gene (see Fig. 4, section 3.4 and Discussion). Panel B: Phylogenetic conservation of putative transcription factor binding sites between mouse promoter described here along and the previously characterized human *ATPase II* promoter (variant I of the human promoter; AY775564, [22]) determined by DiAlingTF ([35-37]; http://www.genomatix.de/online_help/help_dialign/dialign_TF.html). Clusters of phylogenically conserved potential TF binding sites are in boldface in the sequence on Panel A and their locations relative to the TSS are indicated above the sequence. Information on potential TF binding sites found within clusters is included in three tables with and includes matrix names, description of TF, strand at which binding is predicted and location of a potential site relative to the TSS. Please refer to the help MatInspector help page (http://www.genomatix.de/online_help/help_matinspector/matrix_help.html) for further details. Additional TFs identified within the promoter are listed in Supplementary Table I.

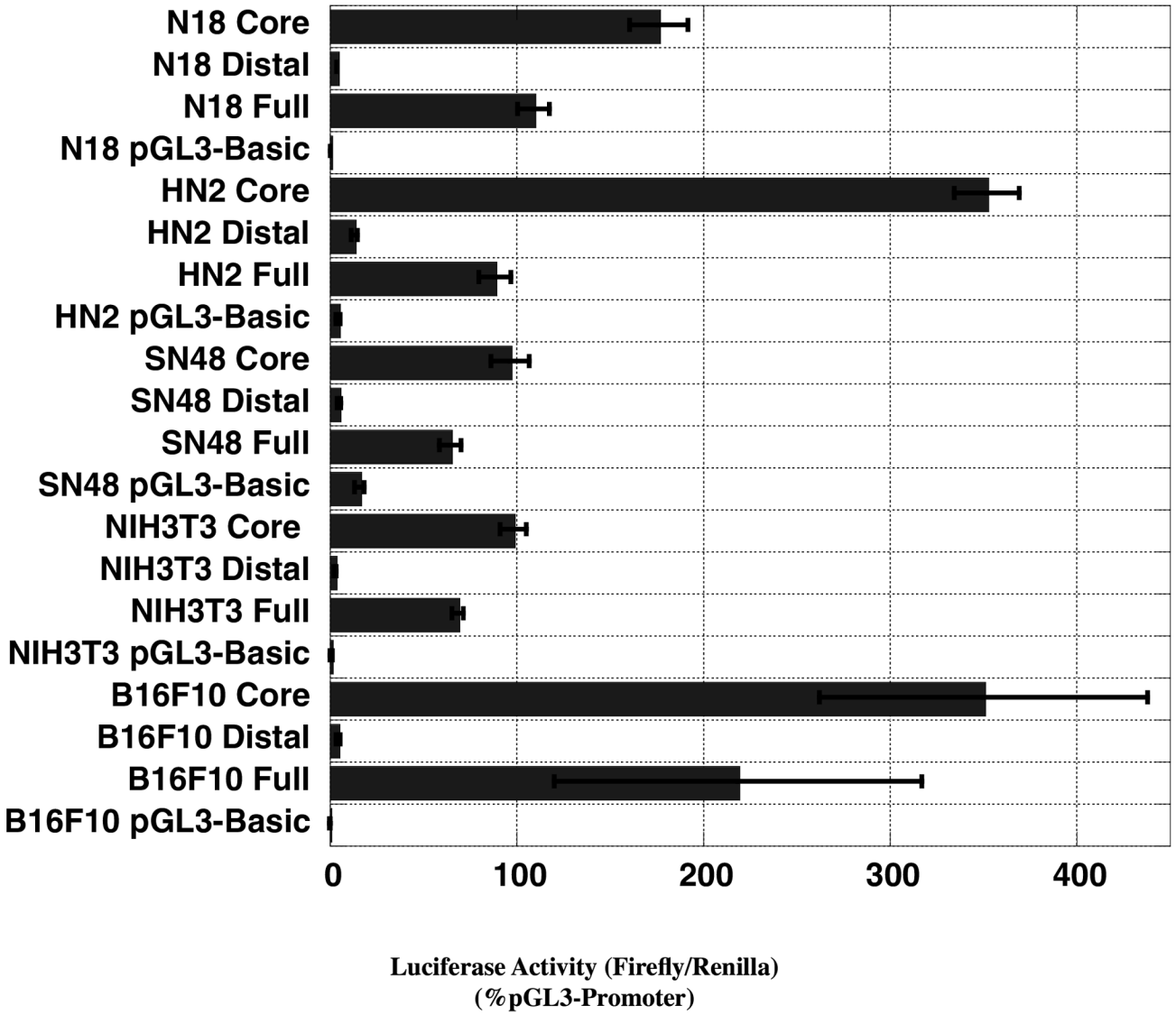

Figure 2.

Transcriptional Activity of the Mouse *ATPase II* promoter (full promoter) and its segments. Either the entire *ATPase II* promoter ('full promoter') or its core or distal parts described in Fig. 1A were obtained using appropriate primers as detailed in Table I and then ligated into the luciferase reporter vector pGL3-Basic. The figure shows luciferase activity of the three promoter fragments transfected into different cell lines. Results obtained upon transfection of the pGL3-Basic promoterless 'empty' vector serve as negative controls. The data have been normalized to the activity of the pGL3-Promoter vector. Data shown represent two independent experiments with the luciferase activity of each deletion mutant measured in quintuplicate. Statistical analysis revealed that in all cell lines transcriptional activity of the distal promoter was not significantly different from that of pGL3-Basic ($P \approx 0.2\text{-}1$).

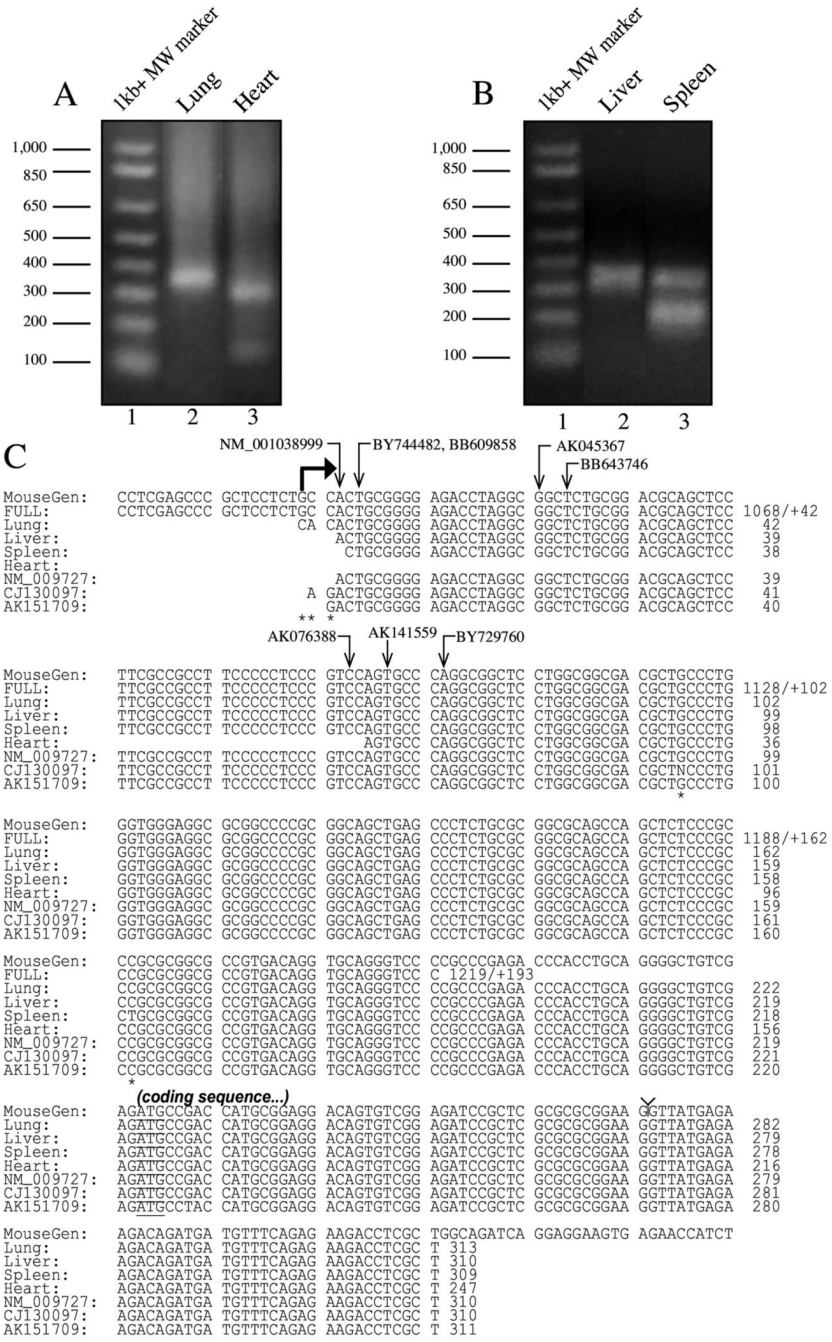

Figure 3.

Comparison of mouse ATPase II 5′RACE products from different tissues with the 5′ ends of mouse ATPase II cDNA sequences obtained from public databases. (A,B) Secondary 5′RACE products obtained using GeneRacer™ 5′ Nested Primer and 5RNestedGSP (Table I) are shown. We have cloned and sequenced the single products obtained from lung and liver cDNA as well as higher molecular weight products only from heart and spleen. (C) Analysis of the sequences of the 5′RACE products obtained from lung, heart, liver and spleen. All mouse 5′RACE products from this figure have been deposited into Genbank and their accession numbers are: lung DQ503477, heart DQ503478, liver DQ503479 and spleen DQ503480. Transcription start sites of the ATPase II clones available from public databases are included. All cDNA clones

the accession numbers of which are shown on this panel as well as on the Supplementary Table II have been reported by authors who submitted their sequences as either full-length or complete at their 5′ends. For the purpose of clarity and brevity, the sequences of only three clones from databases are shown. The 5′ ends of the remaining clones analyzed is denoted by arrows above the sequence. The boldfaced forward-pointing arrow (➪) denotes transcription start site referred to as +1 in the presented studies. The (♈) symbol denotes exon-intron-exon junction between exons 1 and 2 (also refer to Supplementary Table III). '**FULL'** denotes the mouse *ATPase II* promoter described in the present studies bases 1018-1219 (i.e. -18/+193 relative to the TSS) **MouseGen** denotes a mouse *ATPase II* gene sequence obtained from the mouse genome browser version of February 2006: chromosome 5, reverse strand 68,126,587-68,126,297 (the first exon) followed by bases 68,093,858-68,093,790 (5′ end of the second exon, see also Supplementary Table III). In MouseGen sequence only sequences of gDNA that correspond to exon parts are shown and the sequence of the intron between exons 1 and 2 (Supplementary Table III) is not included. Asterisks below sequences denote the region within DNA sequences where at least one of the sequences within the alignment differs from the remaining sequences.

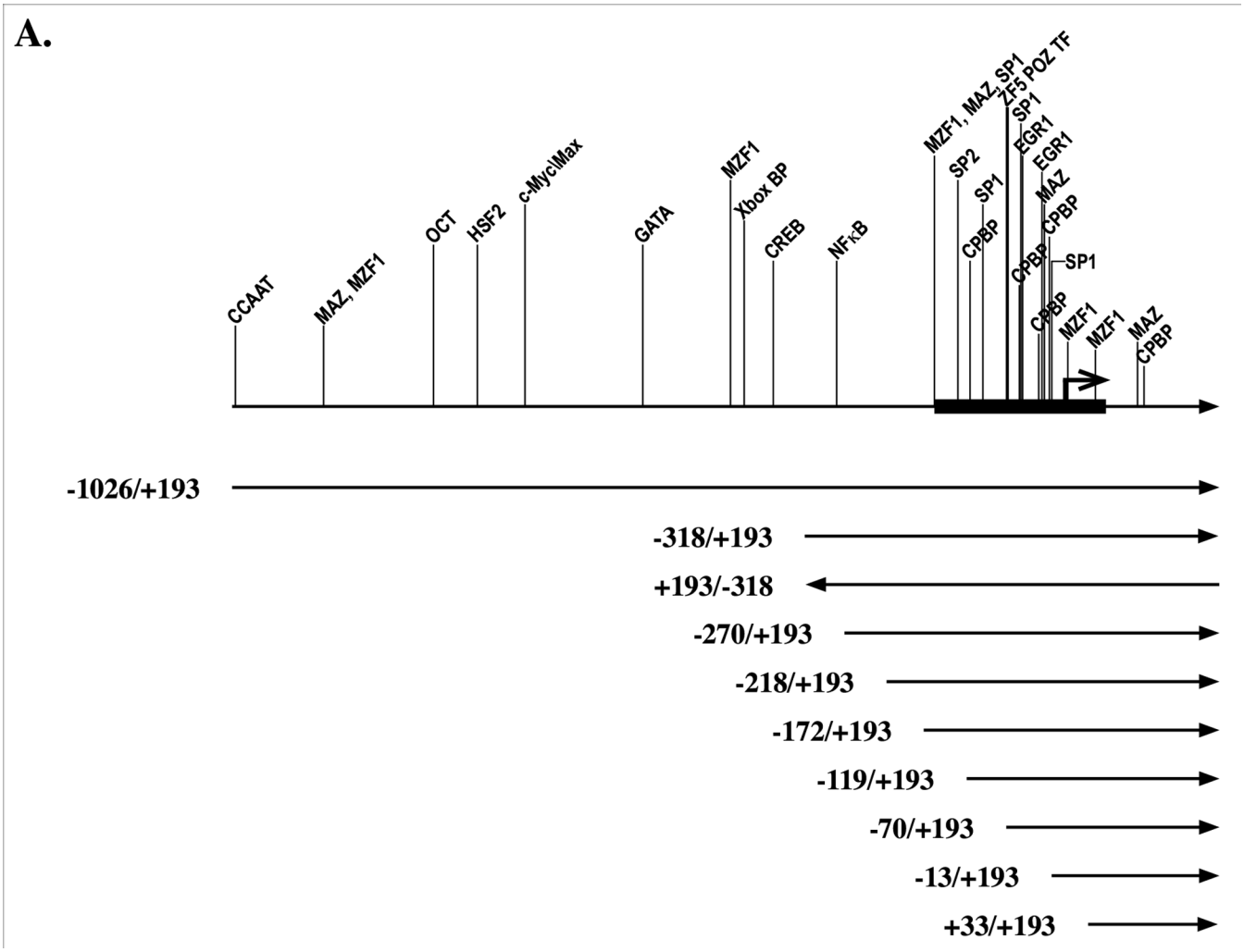

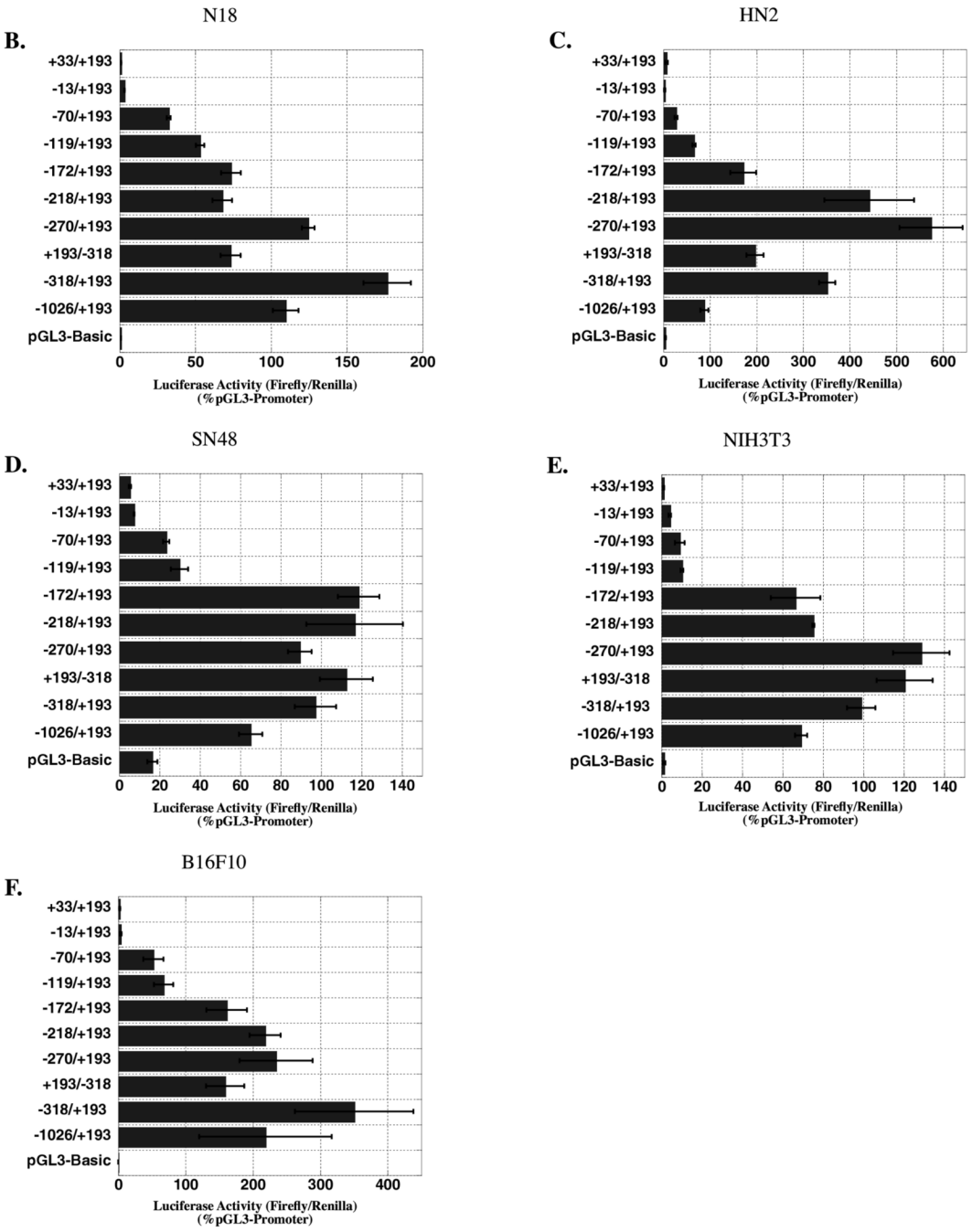

Figure 4.

Deletion analysis of the mouse *ATPase II* promoter. (A) Schematic representation of deletion mutants generated for this study (Abbreviations used: BP-binding protein, BS-binding sites). The thick horizontal line on the topmost panel indicates the promoter detected by PromoterInspector. The reporter luciferase gene is shown as a box with a black arrowhead. The ATPase II deletion mutants are schematically shown as thin lines with arrows. The direction of an arrow at either the beginning (all mutants except the +193/-318) or the end of the line (+193/-318) corresponds to the direction in which the mutant was cloned with respect to the luciferase reporter gene. (B-F) Luciferase activity of the promoter constructs transfected into different cell lines. Data shown represent two independent experiments with the luciferase

activity of each deletion mutant measured in quintuplicate. The results have been normalized to the activity of the pGL3-Promoter vector.

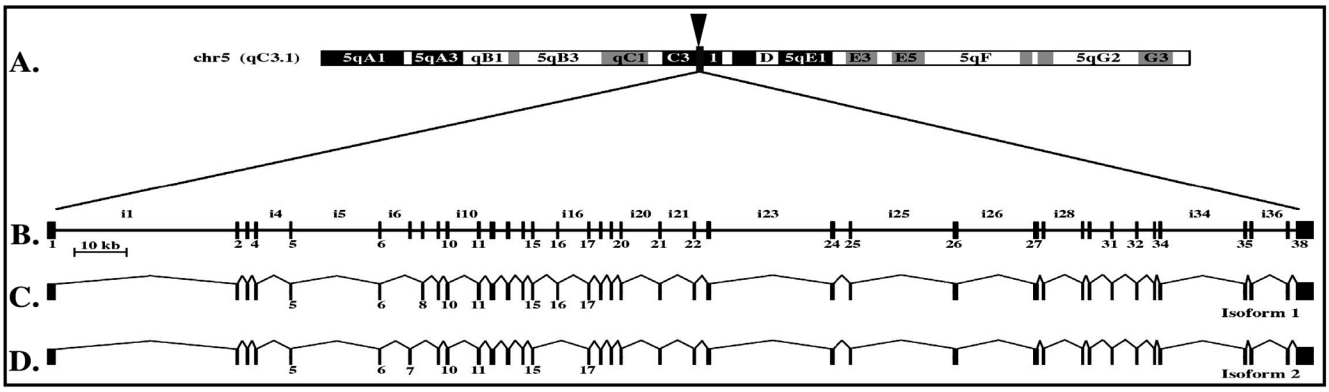

Figure 5.

Chromosomal localization including gene structure of the mouse *ATPase II* and two types of transcript variants produced by alternative splicing. The gene structure has been drawn to scale. The panels are from top to bottom: (A) schematic illustration of mouse chromosome 5 as interpreted by the mouse genome browser, (B) intron-exon organization of the *ATPase II* gene, two transcript variants 1 and 2 (panels C and D respectively) which are results of alternative splicing of exons 6, 7 and 16. The arrowhead at the top of the figure indicates the position of the *ATPase II* gene. Exons are indicated by thin vertical lines.

Table I

Primers used in various stages of the project.

Name	Sequence (5' to 3')	Method used for:	Comments
ATPaseFORW (−1026sns)*	*CGG* GGT ACC AAA GCC TTG CTA CAG GCT CTT TCC G	Primers used for initial amplification of the putative *ATPase II* promoter (shown in sections 3.1, 3.2, and Fig. 1).	
ATPaseRev (+193ants)*	*CTA* GCT AGC GGG ACC CTG CAC CTG TCA CG		
DistalRev (−229antsns)*	*CTA* GCT AGC CAA TGC GAT AGA ACC GAC CGT CC	The *ATPase II* Distal Promoter (see section 3.2) amplified using this primer and **ATPaseFORW(−1026sns).**	
CoreFORW (−318sns)*	*CGG* GGT ACC CGG TCG GTT CTA TCG CAT TGT AGA GC	Generation of serial deletions of the *ATPase II* promoter. Serial deletions were generated using foward **('sns')** primers and **ATPaseRev (+193antsns)** reverse primer. Each primer contained either a KpnI or NheI site in order to facilitate recloning into pGL3 Basic vector in a sense orientation (see section 2.4). Recloning of products obtained using −318sns-NheI and +193antsns-KpnI resulted in the core promoter being placed in pGL3 basic in an antisense orientation.	Primers designed based on sequencing of the full promoter along with mouse genomic sequence available from the Mouse Genome Project Draft freezes between November 2001 and May 2004.
−270sns	*CGG* GGT ACC CAG AGC TTT CAG AGC TAA AGA AGC		
−218sns	*CGG* GGT ACC ACT TGT ACT GGC CTC AAG GAG G		
−172sns	*CGG* GGT ACC AAT GCT AGA TCG AAG TCC CCT CC		
−119sns	*CGG* GGT ACC ACC TGG AGG CTC GGC GGC CCT GTC C		
−70sns	*CGG* GGT ACC AGT GAG CGC GCG CCC CGC AGA CC		
−13sns	*CGG* GGT ACC AGC CCG CTC CTC TGC CAC TGC		
+27sns	*CGG* GGT ACC ACG CAG CTC CTT CGC CGC CTT CC		
−318sns-NheI	*CTA* GCT AGC CGG TCG GTT CTA TCG CAT TGT AGA GC		
+193antsns-KpnI	*CGG* GGT ACC GGG ACC CTG CAC CTG TCA CG		
5RGSP	GCA GCT CTT CTG AAC TGA GAG TAG AGA AAT C	RLM-RACE (primary amplification), selected bp 230...200 upstream of ATG within exon 3.	Primers designed based on sequence of the ATPase II RefSeq NM_009727 and the organization of the *ATPase II* gene (Fig. 5, Supplementary Table III).
5RNestedGSP	TGG GGC TGG TTG ATG AAA ATA GTC C	RLM-RACE (secondary amplification), selected bp 134...110 upstream from ATG, exon 2.	
GeneRacer™ 5' Primer	CGA CTG GAG CAC GAG GAC ACT GA	RLM-RACE (primary amplification), binding site for this primer was located within the GeneRacer™ RNA Oligo.	Primers Provided in the GeneRacer™ kit.
GeneRacer™ 5' Nested Primer	GGA CAC TGA CAT GGA CTG AAG GAG TA	RLM-RACE (secondary amplification), binding site for this primer was located within the GeneRacer™ RNA Oligo.	

*These primers were used in our initial studies described in sections 3.1 and 3.2 and were given generic names -FORW or -Rev. Subsequently, once transcription start sites for the *ATPase II* promoter were identified (section 3.2) names of theses primers were changed to maintain the same naming system for all the primers used in promoter deletion studies (section 3.4).